ELSEVIER

Understanding CYP2D6 interactions

Marcel J. de Groot[1], Florian Wakenhut[1], Gavin Whitlock[1] and Ruth Hyland[2]

[1] World Wide Medicinal Chemistry (WWMC), United Kingdom
[2] Pharmacokinetics, Dynamics and Metabolism (PDM), United Kingdom

Owing to the polymorphic nature of CYP2D6, clinically significant issues can arise when drugs rely on that enzyme either for clearance, or metabolism to an active metabolite. Available screening methods to determine if the compound is likely to cause drug–drug interactions, or is likely to be a victim of inhibition of CYP2D6 by other compounds will be described. Computational models and examples will be given on strategies to design out the CYP2D6 liabilities for both heme-binding compounds and non-heme-binding compounds.

Introduction

Cytochromes P450 (P450s, CYPs [1,2]) constitute a large superfamily of heme-containing enzymes. This superfamily is divided into families for which the pairwise amino acid sequence identity between individual members is >40%, and then into subfamilies for which the pairwise amino acid sequence identity between members is usually ≥55% [2]. P450s can metabolize (either oxidize or reduce) a large number of structurally different endogenous and exogenous compounds [3]. Seven of the 57 known human isoforms of P450s are responsible for more than 90% of the metabolism of all pharmaceuticals in current clinical use: CYP1A2, CYP2C9, CYP2C18, CYP2C19, CYP2D6, CYP2E1, and CYP3A4 [4] Several of the P450 isoforms display polymorphisms (e.g. CYP2D6, CYP2C9) that can result in the poor metabolism of drugs [5].

Cytochrome P450 2D6 (CYP2D6) is one of the polymorphic members of the P450 superfamily and is absent in ~7% of the Caucasian population (PM, poor metabolizers). There is also a population that has expression of multiple genes leading to the Ultrarapid Metabolizer phenotype (UM) that is present in ~3% of the Caucasian population and 20–29% in Saudi Arabia/Ethiopia [6,7]. Currently, >50 different human genetic variations have been identified, several of which are inactivating alleles [8], which result in a deficiency in drug oxidation known as the debrisoquine/sparteine polymorphism, affecting the metabolism of numerous drugs. No definitive disease linkage has been associated with either gene deletion/inactive enzyme or enzyme overexpression [9,10]. CYP2D6 accounts for ~5% of active P450 in human liver, but metabolizes 20–25% of known drugs, which gives rise to the potential for increased drug–drug interactions (DDIs), when co-medications are 2D6 substrates [11].

The known substrates of CYP2D6 represent a variety of chemical structures, common characteristics being the presence of at least one basic nitrogen atom, a distance of 5 Å or 7 Å between the basic nitrogen atom and the site of oxidation, a flat hydrophobic area near the site of oxidation and a negative molecular electrostatic potential (MEP) above the planar part of the molecule [12–14]. However, several substrates with a distance of approximately 10 Å between the basic nitrogen atom and the site of oxidation are known [15], and likewise substrates where metabolism takes place next to the basic nitrogen atom [16].

Assessing risk: measuring CYP2D6 metabolism and inhibition

An estimated 20–25% of all drugs in current clinical use are metabolized to some degree by CYP2D6. Ultrarapid metabolizers will clear the body of CYP2D6 substrates more rapidly, and consequently the potential for subtherapeutic plasma levels in this group is higher, and dosing adjustments may be required to achieve the required efficacy [17–19]. Poor metabolizers, those subjects without functional CYP2D6 enzyme, clear CYP2D6 substrates more slowly and therefore may have increased plasma exposure to those drugs, thereby giving rise to an increased

Corresponding author: de Groot, M.J. (marcel.degroot@pfizer.com)

1359-6446/06/$ - see front matter doi:10.1016/j.drudis.2009.07.005

TABLE 1

Overview of a representative set of models available for CYP2D6

Model	Description	Ref
Pharmacophore	Manual alignment based on substrates with a basic nitrogen atom 5 Å from site of oxidation and coplanar aromatic rings.	[55]
Pharmacophore	Manual alignments based on substrates with a basic nitrogen atom 7 Å from site of oxidation and coplanar aromatic rings.	[56]
Pharmacophore	Model using 15 substrates suggesting a distance between basic nitrogen atom and the site of oxidation between 5 and 7Å.	[57]
Pharmacophore	Model based on 19 substrates. Site of oxidation 5–7 Å from basic nitrogen, can be combined with inhibitor model [12,52].	[52]
Pharmacophore	Model using six potent reversible inhibitors. Can be combined with pharmacophore for substrates [52].	[12,52,53]
Pharmacophore	Model based on substrates suggesting a hypothetical carboxylate group to be responsible for the distance of either 5 Å or 7 Å between basic nitrogen atom and site of oxidation in the substrate.	[13,58,59]
Pharmacophore	Model based on previous pharmacophore models, utilizing the same substrates [13,58,59], incorporating the positions of the heme moiety and the I–helix (containing Asp^{301}) of a CYP2D6 comparative model [46].	[14]
Pharmacophore embedded in comparative model	Pharmacophore models for substrates constructed within the active site of a comparative model (based on bacterial P450 X-ray structures). Model consists of two pharmacophores (describing O–dealkylation and oxidation reactions and *N*-dealkylation reactions, respectively) embedded in a comparative model.	[15,16]
Pharmacophore embedded in comparative model	Pharmacophore models for substrates and fitted into the active site of a comparative model (based on bacterial P450 X-ray structures.	[60]
QSAR: 3D and 4D	Model based on 20 inhibitors of bufuralol 1′-hydroxylation.	[61]
QSAR: 3D and 4D	Model based on 31 K_i values. Predicted K_i values for 10 out of 15 CYP2D6 inhibitors within one log residual. Model was used successfully predict the CYP2D6 inhibitory potency of three components of St. John's Wort [62].	[61]
QSAR: RP	Recursive partitioning model (RP, decision tree) using commercial data set of 1750 compounds, predicting CYP2D6 inhibition, enabling statistical significant rank ordering of a set of test molecules/	[63]
QSAR: NN	Neural Network (NN) models for CYP2D6 mediated *N*-dealkylation.	[64]
QSAR: RP	A variety of Recursive Partitioning (RP < decision tree) models for CYP2D6 with >80% accuracy	[65]
QSAR: PLS and RP	Partial Least Square (PLS), Recursive Partitioning (RP, decision tree) and combined PLS + RP models based on 170 compounds, validated with 89 compounds, using various descriptor sets	[66]
QSAR: kNN	CYP2D6 inhibition k-nearest neighbor (kNN) model based on 1153 compounds. Classifies 82% of compounds correctly.	[67]
QSAR: PLS	Partial Least Squares (PLS) model for CYP2D6 metabolic stability using 3-point pharmacophore fingerprints and comparison with other descriptors.	[68]
QSAR	QSAR model for CYP2D6 inhibition based on 33 curcumin analogues.	[69]
QSAR: 2D and 3D	QSAR models for inhibition of CYP2D6 by aryloxypropanolamines.	[70]
Homology	On the basis of bacterial CYP102 crystal structure.	[48]
Homology	On the basis of on bacterial CYP101, CYP108 and CYP102 crystal structures and NMR restraints.	[47]
Homology	On the basis of bacterial CYP101, CYP108 and CYP102 crystal structures.	[15,45,46]
Homology	On the basis of rabbit CYP2C5 crystal structure.	[50]
Homology	On the basis of (CYP101, CYP108, CYP102, CYP107A and CYP2C5). Used for automated docking.	[49,71]
Homology and Molecular Dynamics	Automated docking and Molecular Dynamics of CYP2D6 substrates in a CYP2D6 homology model.	[72]
Homology and CoMSiA	Homology model based on rat CYP2C5 crystal structure, in combination with CoMSiA (comparative molecular similarity index analysis) for CYP2D6 inhibitors.	[73]

potential for drug-induced adverse events (AEs) [17–19]. There have been a number of studies investigating the potential for increased adverse events in the CYP2D6 PM population. For example, a study with the HMG–CoA reductase inhibitor simvastatin [20] found an association between CYP2D6 polymorphism and both efficacy and tolerability. CYP2D6 polymorphism has been shown to have a significant effect on adverse event rates and dosing regime in the area of anti-psychotic medication [21,22]. A linkage between CYP2D6 genetic variation and lower heart rate and blood pressure effects in β-blocker users has recently been demonstrated, giving an increased risk of bradychardia in CYP2D6 PMs [23]. An alternative risk in the PM population is reduced efficacy where a drug requires metabolism to an active metabolite via CYP2D6. For example, the anti-cancer drug tamoxifen is metabolized to an active metabolite by CYP2D6, and therapeutic responses in CYP2D6 PMs have been found to be smaller than the extensive metabolizer (EM) population [24].

The above examples highlight the clinically significant issues that can arise in the CYP2D6 PM population when drugs rely on that enzyme either for clearance, or metabolism to an active metabolite. As a consequence there has been a significant effort in pre-clinical drug discovery to ensure that drug candidates are not potent inhibitors of CYP2D6, since agents with this property have the potential to be perpetrators of drug–drug interactions (DDI) when co-dosed with CYP2D6 substrates. Additionally it is desirable to avoid significant metabolism by CYP2D6, thus reducing the potential for those drugs to be victims of DDIs when co-dosed with a CYP2D6 inhibitor.

Predicting risk from *in vitro* data

Throughout the drug discovery and development process it is important to understand the DDI risk for a new chemical entity (NCE). Figure 1 illustrates the step-wise approach typically followed when assessing the DDI risk.

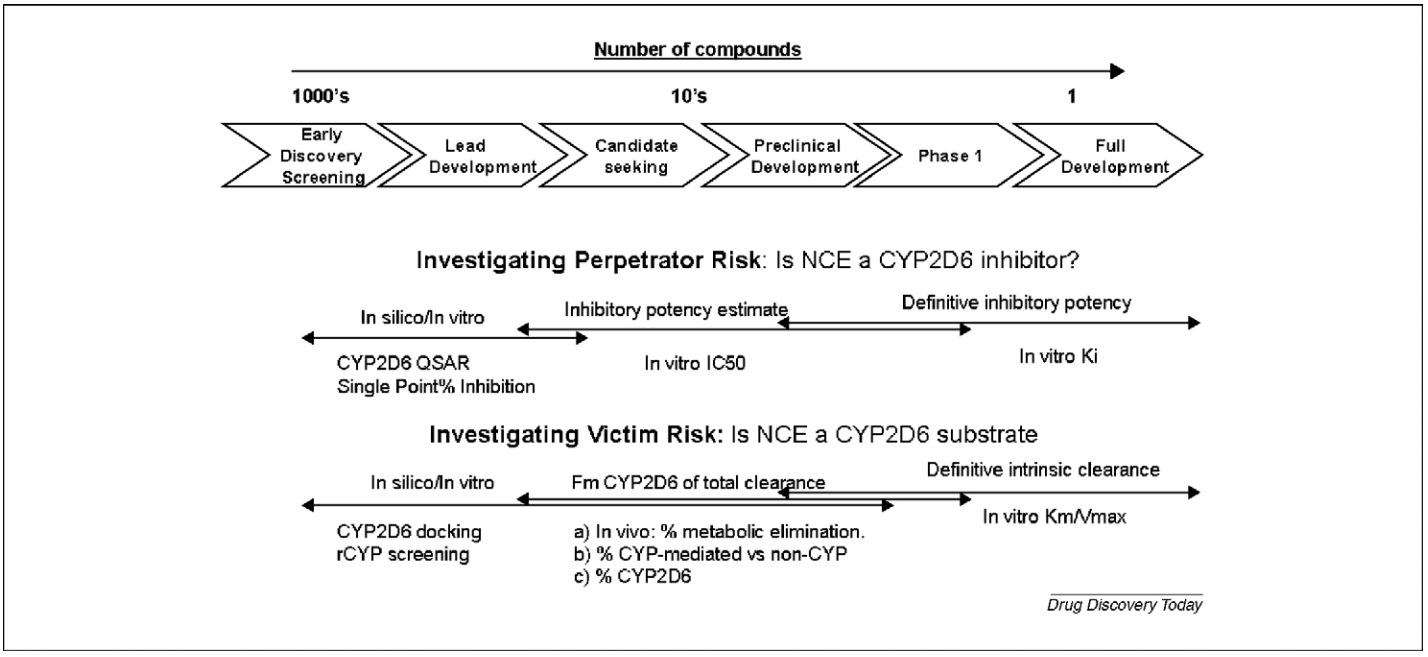

FIGURE 1

Step-wise approach typically followed when assessing the DDI risk.

In recent years, the utility of *in vitro* data to predict *in vivo* pharmacokinetics (PK) and DDI for CYP2D6 substrates and inhibitors has been demonstrated [25,26]. Whether assessing a NCE as a potential perpetrator of an interaction or a potential victim the same principles are applied. The equation described by Rowland and Matin [27] forms the basis of this approach:

$$\text{magnitude of DDI} = \frac{\text{AUC}_{\text{inhibited}}}{\text{AUC}_{\text{control}}} = \frac{1}{(f_{\text{CL}}/(1+([I]_{in}/\text{K}_\text{i}))) + (1-f_{\text{CL}})} \quad (1)$$

where $\text{AUC}_{\text{inhibited}}$ and $\text{AUC}_{\text{control}}$ refer to the exposures when co administered and not co administered with a second drug, respectively; f_{CL} refers to the fraction of clearance that is mediated by the enzyme that is affected; K_i is the reversible inhibition constant and $[I]_{in\ vivo}$ is the concentration of the inhibitor available to bind to the affected enzyme *in vivo*. Estimates of unbound portal vein concentration for $[I]_{in\ vivo}$ have been shown to be useful in predicting DDI for reversible inhibitors [28,29].

Perpetrator interactions

For predicting whether an NCE will be a perpetrator of DDI, defining K_i from *in vitro* assays is required. For reversible inhibition, a general rule-of-thumb states that compounds with inhibition potencies less than 1 μM tend to more frequently cause DDI [30,31] and a competitive inhibition screen based upon the IC_{50} principle is often the first step in understanding the DDI potential of a NCE. The relationship between K_i and IC_{50} for a competitive inhibitor is

$$\text{IC}_{50} = \text{K}_\text{i}\left(1+\frac{[S]}{\text{K}_\text{m}}\right) \quad (2)$$

Under assay conditions whereby the concentration of the probe substrate is equivalent to K_m, an IC_{50} estimate is equivalent to twofold K_i. For non-competitive inhibition, K_i is equivalent to IC_{50} since inhibitor and substrate binding are independent. Two DDI screens, the conventional inhibition screen and the fluorescent inhibition screen, are commonly used and simplifying the experimental system by using a single point inhibitor concentration reduces the number of samples and allows for a higher throughput assay. Typically drug concentrations in the 1–5 μM range are used [32,33]. An estimated IC_{50} can be determined by fitting the average percent control activity into a model [33,34]. Compounds of interest may be followed up with the DDI multipoint determination to enable determination of an IC_{50}. From equation 2 an estimate of K_i can be used for incorporation into equation 1 for prediction of DDI, or the definitive K_i may be determined.

The DDI conventional inhibition screen utilizes a specific probe substrate, typically dextromethorphan or bufuralol for CYP2D6, which may be investigated alone, or in a cocktail with other P450 probes [35,36] and the amount of metabolite formed from the probe substrate is measured relative to the uninhibited wells using LC/MS/MS detection. The assay is moderate throughput and can support a few hundred compounds per week. The DDI fluorescent inhibition screen is a high throughput screen, primarily as a result of reduced analysis time, and can range from a few hundred to a thousand compounds per week. The assay uses recombinant CYP2D6 with a fluorogenic substrate (3-[2-(*N*,*N*-diethyl-*N*-methylamino)ethyl]-7-methoxy-4-methyl-coumarin (AMCC), or Vivid® EOMCC) but is more prone than the conventional inhibition screen to NCE interferences within the assay (i.e. inherently fluorescent NCEs, fluorescent quenching by the NCE). While the DDI fluorescent screen has the benefit of being relatively simple and inexpensive, with the ability to bin compounds (low, medium, high risk), caution does need to be taken when fluorescent data are used to drive decision making for DDI owing to known differences in inhibitory potencies that can be observed between the fluorescent screen and the conventional screen [37].

For this reason IC_{50} and K_i determinations using conventional probes are preferred for quantitative prediction of DDI risk.

Victim interactions

For the NCE as a victim of inhibition by other compounds, *in vitro* data to predict f_{CL} are crucial and once this is obtained, predictions of DDI using standard perpetrators, such as quinidine, can be made. An estimate for f_{CL} by CYP2D6 can be obtained using a three tiered approach [29]. Firstly an assessment of the fraction of clearance that occurs by metabolism is made by examining the amount of unchanged drug excreted in the urine and bile of laboratory animals. Secondly, the fraction of metabolic clearance mediated by P450 enzymes vs. other drug metabolizing enzymes is estimated by *in vitro* assays in the presence and absence of 1-aminobenzotrazole (ABT), a chemical tool that can serve as a pan-P450 inactivator [38]. Finally, the fraction of P450 metabolic clearance that will be mediated by CYP2D6 can be determined through reaction phenotyping experiments using the approaches (a) or (b) outlined below:

(1) Human liver microsomes in combination with specific P450 inhibitors (or inhibitory antibodies), whereby the metabolic rate constants in the presence ($k_{(I)}$) and absence (k) of chemical inhibitors are used to calculate the percentage of contribution of each P450 enzyme to the *in vitro* metabolism of the test compound (using equation 3) and subsequently the f_{CL} for each P450 is determined.

$$\%\,\text{contribution} = \frac{(-k) - (-k_{(I)})}{(-k)} \qquad (3)$$

or

(2) Individual Cl_{int} in recombinant P450 enzymes can be scaled to the corresponding Cl_{int} values for that P450 in human liver microsomes [39] by use of relative activity factors (RAF) [40,41], or intersystem extrapolation factors (ISEFs) that combine the RAF approach with relative P450 abundance. The f_{CL} by CYP2D6 can then be estimated from the sum of the total scaled Cl_{int}. This value is incorporated into equation 1 and an assessment of risk when administered in combination with a CYP2D6 inhibitor can be made. In addition, the same *in vitro* data can be used to evaluate the risk associated with administration of a CYP2D6 substrate to a CYP2D6 poor metabolizer population. Of particular value here is the Simcyp population-based ADME simulator [42] that simulates pharmacokinetics in representative virtual populations on the basis of the *in vitro* data. The software incorporates numerous databases containing human physiological, genetic and epidemiological information. By integrating this information with the *in vitro* data, the simulator allows the prediction of pharmacokinetic behavior with the added benefit of information on expected population variability. The utility of the simulator is exemplified by the work of Dickinson and coworkers [43] who demonstrated the ability to model differences in the pharmacokinetics and pharmacodynamics of dextromethorphan between CYP2D6 poor and extensive metabolizer phenotypes. The simulations indicated that about five subjects would be adequate to achieve 80% power to detect a significant difference in the AUC of dextromethorphan between the 2 CYP2D6 phenotypes while a power of 100% was obtained when comparing 22 EMs with 22 PMs.

Finally, it is important to note that while the predicted fold change in AUC is an important descriptor of risk, this value should not be considered in isolation. Depending on the pharmacological and toxicological profile of the NCE there may be instances whereby a large predicted increase in AUC can be tolerated. Likewise, for a substrate with a low therapeutic index, even a small predicted change in AUC may be considered too great a risk for progression of the compound.

Predicting risk: models, predictions and crystal structures

Before the appearance of crystal structures of mammalian P450s [44], homology models were constructed for various P450s including CYP2D6 [15,45–50] (see Table 1). One of these models was a combined pharmacophore model embedded in a homology model [15,16]. The homology model showed interactions between Arg^{132}, His^{376}, Ser^{413} and Arg^{441} and the propionate groups of the heme moiety, while Asp^{301}, Glu^{216} and Phe^{481} were proposed as key residues in the active site. The model contained a hydroxylation pharmacophore, based on 57 metabolic pathways in 40 CYP2D6 substrates that had their basic nitrogen, site of oxidation and the planar region overlaid, and an *N*-dealkylation pharmacophore, which encompassed 15 *N*-dealkylation pathways in 14 substrates, overlaying the sites of oxidation and the planar region of the molecules. More recently a crystal structure of CYP2D6 became available [51], finally allowing a validation of the models. For the model described above, the main differences with the crystal structure were in the loop between helices F and G and the B–C loop region, which is pushed outward in the crystal structure. Of the predicted key interacting amino acids, $Asp^{301}$and Glu^{216} were in agreement, while the location of Phe^{481} in the model is occupied by Phe^{483} in the crystal structure, coming in from a different angle, showing that the alignment used to build the model was not perfect. Despite this difference, the charge distribution and sterics in the binding site are very similar between model and crystal structure and more importantly, both pharmacophores from the model can be accommodated within the crystal structures of CYP2D6 with minor only steric clashes caused by sidechains, which was expected as the crystal structure is an apoform (Figure 2A). The clashing amino acid side chains can move away slightly to accommodate the entire pharmacophores without forcing the protein into a much higher energy conformation.

Interactions between compounds from the pharmacophore model with the amino acids of the crystal structure are: Phe^{219} (long range), Leu^{248} (long range), Phe^{120}, Asp^{301}, Glu^{216} and Phe^{483} (not Phe^{481}) as shown in Figure 2B.

The pharmacophore models derived within the homology model can be accommodated within the crystal structure, explaining why the model was successful in helping design out CYP2D6 metabolism in Drug Discovery projects, years before a crystal structure was available.

Modeling inhibitors in the active site is slightly more difficult as inhibitors lack the site of oxidation used in modeling. Inhibitors can bind in a similar region as substrates, as was suggested by an early model [12,52,53], and from recent crystal structures with bound inhibitors for CYP2C9 [54]. However, inhibitors do not

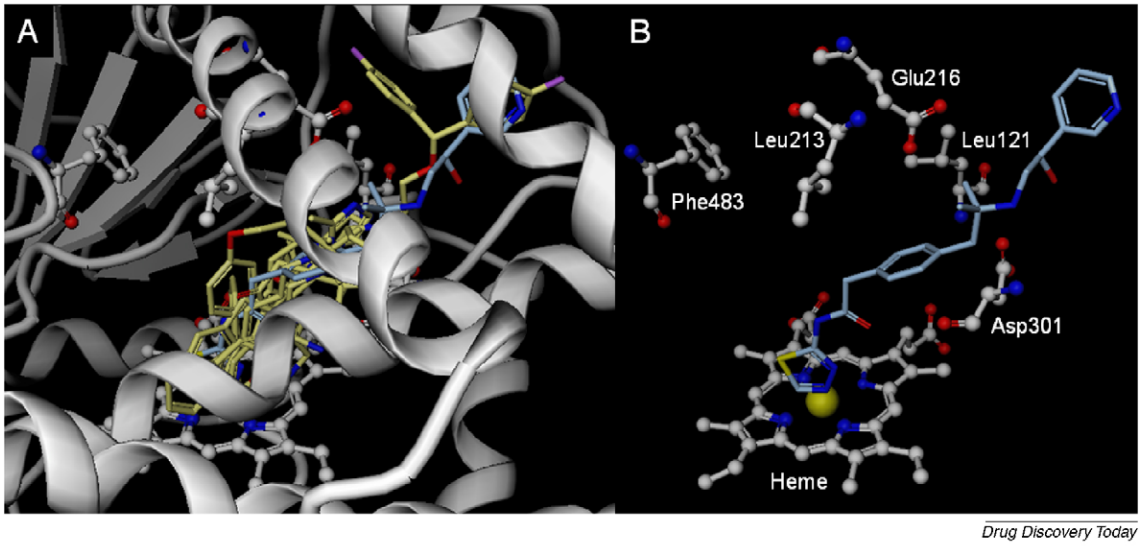

FIGURE 2

A: CYP2D6 pharmacophores developed within the active site of the CYP2D6 model [15,16] placed within the active site of the CYP2D6 crystal structure showing the overlap of **1** with a representative set of compounds from the CYP2D6 substrate pharmacophore (dextromethorphan, debrisoquine, ondansetrone, metoprolol, GBR12909, bufuralol, amytriptyline, and tropisetron) [51]. B: Active site residues of the CYP2D6 crystal structure shown flanking **1** (see Figure 3).

have to bind in the same region as substrates since they can inhibit by blocking the access channel for substrates or bind in other parts of the active site, limiting accessible space for substrates near the heme.

Designing out CYP2D6 interactions: examples from Pfizer drug discovery programs

The following discussion is intended to illustrate potential options for the medicinal chemist to consider when confronted with CYP2D6 interaction issues but is not comprehensive.

CYP2D6 inhibition

CYP2D6 inhibition and compound classes

An analysis of a comprehensive data set comprising Pfizer and literature compounds (~3500 compounds) demonstrated that:

(i) 2D6 inhibition is primarily an issue for basic compounds. Indeed, in this data set basic compounds represented >92% of compounds exhibiting 2D6 IC_{50} <1 μM compared with only 7% for neutrals.

(i) 22% of all the basic compounds exhibited 2D6 IC_{50} <1 μM (total count: 2675) compared with 6% of neutrals (total count: 738), 4% of zwitterions (total count: 28) and 0% of acids (total count: 88).

(i) Decreasing polarity as measured by topological polar surface area (TPSA) generally resulted in greater CYP2D6 inhibition for basic and neutral compounds. Indeed, for basic compounds, only 37% of compounds with TPSA >100 $Å^2$ exhibited 2D6 IC_{50} < 10 μM, this percentage increased to 73% for compounds with TPSA < 50 $Å^2$. Increasing lipophilicity as measured by c log *P* also resulted in greater CYP2D6 inhibition for basic and neutral compounds (45% of bases with 1 < c log *P* < 3 exhibited 2D6 IC_{50} < 10 μM, 72% of bases with 3 < c log *P* < 5 exhibited 2D6 IC_{50} < 10 μM).

These findings are consistent with previously reported analyses [61,74,75] and can be rationalized by the presence in the active site of the two key acidic residues Asp^{301}, Glu^{216} and several aromatic residues, that is, Phe^{483} or Phe^{481}, all potentially acting as key binding residues for the inhibitors [51].

Designing out CYP2D6 inhibition

As described above, inhibitors can bind in a similar region as substrates. In this case, a heme-binding group is often present in a similar location as the site of oxidation in substrates. However, inhibitors can also bind in other parts of the active site, either blocking the access channel for substrates or limiting accessible space for substrates near the heme. Strategies for reducing CYP2D6 inhibition may therefore vary, depending on the binding mode (heme binder or non-heme binder). An example of each scenario will be described in the following discussion utilizing two case studies from drug discovery programs at Pfizer in basic chemical series.

Heme binders

For heme binders, the most effective strategy to design out CYP2D6 inhibition is probably to tackle the specific molecule–iron interaction itself rather than trying to modify the periphery of the inhibitor. This is illustrated by the example in Figure 3. Compound **1** was found to be a potent CYP2D6 inhibitor (91% inhibition at 3 μM). When docked in the active site [15,16], as can be seen in Figure 3, it was found that the aminothiadiazole group could potentially interact with the heme through one of the nitrogen lone pairs. On the basis of this observation, a strategy of making modifications to the aminothiadiazole group resulted in very pronounced differences in CYP2D6 inhibition. For example, substitution of the aminothiadiazole group with a methyl group, affording compound **2**, resulted in a significant loss of activity

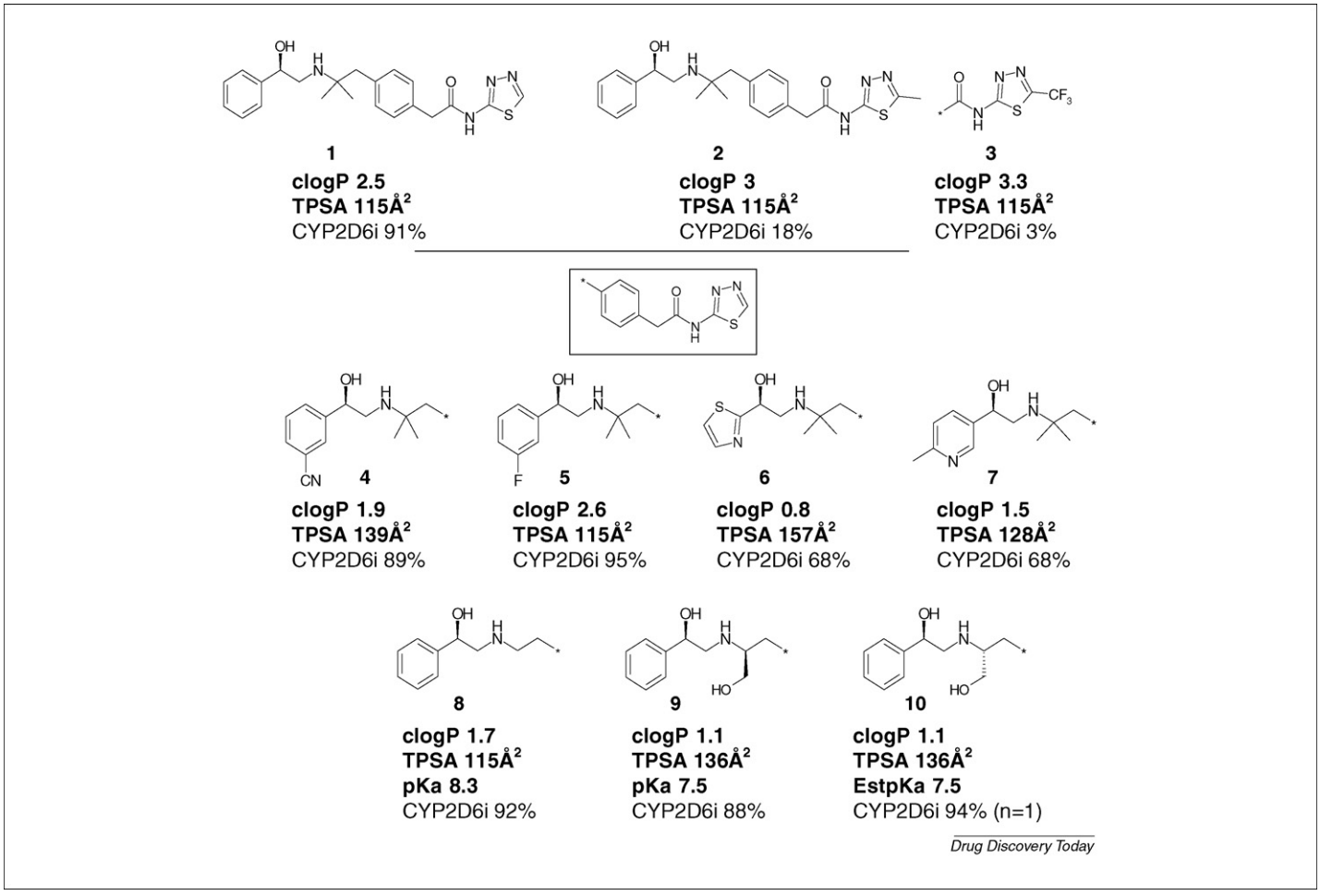

FIGURE 3

Heme binder SAR (CYP2D6 inhibition expressed as %age inhibition at 3 μM, minimum of two experiments).

with only 18% inhibition exhibited at 3 μM, probably as a result of steric clash. A similar result was observed when the aminothiadiazole was substituted by a trifluoromethyl group, affording compound **3**, with only 3% inhibition exhibited at 3 μM. On the contrary, modification of the aromatic substituent of the left-hand-side aminoalcohol while retaining the aminothiadiazole group generally did not lead to significant improvement as illustrated by compounds **4–7** all exhibiting > 65% inhibition at 3 μM, despite variations in c log *P*. We had also already demonstrated, using compound **8** as a starting point, that modifications to the vicinity of the basic amine group in an attempt to disrupt a hypothetical interaction with Asp^{301} or Glu^{216} by modulating p*K*a (compound **8** vs. compounds **9** and **10**) or increasing steric hindrance (compound **1** vs. **8**) gave a similar result.

Finally it is worth noticing that this series does not fit the TPSA and c log *P* trends described in the section above.

Non-heme binders

For inhibitors that are not thought to interact directly with the heme, small modifications to the periphery of the molecule can have a significant impact on inhibition. This is well illustrated with the series of morpholine compounds depicted in Figure 4. For example, swapping a chlorine with a fluorine substituent on the phenoxy **A**-ring resulted in >35-fold drop in potency (compound **12** vs. **11**), while replacing a trifluoromethoxy by a methoxy group resulted in >200-fold drop in potency (compound **13** vs. **14**). Furthermore, introduction of a 5-fluoro substituent on the phenoxy **A**-ring of compound **11** resulted in >13-fold increase in potency while introduction of a 6-fluoro substituent on the phenoxy **A**-ring of compound **13** resulted in ~30-fold decrease in potency. Similar SAR was observed with substitution around the phenyl **B**-ring as can clearly be seen when comparing compounds **17**, **18** and **19** where differences in potency of up to 10-fold were achieved by different fluoro isomers. Finally, replacing the phenyl ring by other heterocycles (compounds **20, 21**) also led to differences in activity.

Although it is difficult to wholly rationalize these experimental findings, several explanations, individually or in combination, can be formulated including for example (i) differences in structure/conformation, (ii) differences in physico-chemical properties, notably lipophilicity, (iii) specific interactions with residues in the active site.

CYP2D6 metabolism

There are few well-validated strategies for reducing the degree of which a drug candidate is metabolized by CYP2D6. In a published Pfizer example, blocking the CYP2D6 mediated pathway was investigated [76]. Although this approach sounds rather obvious,

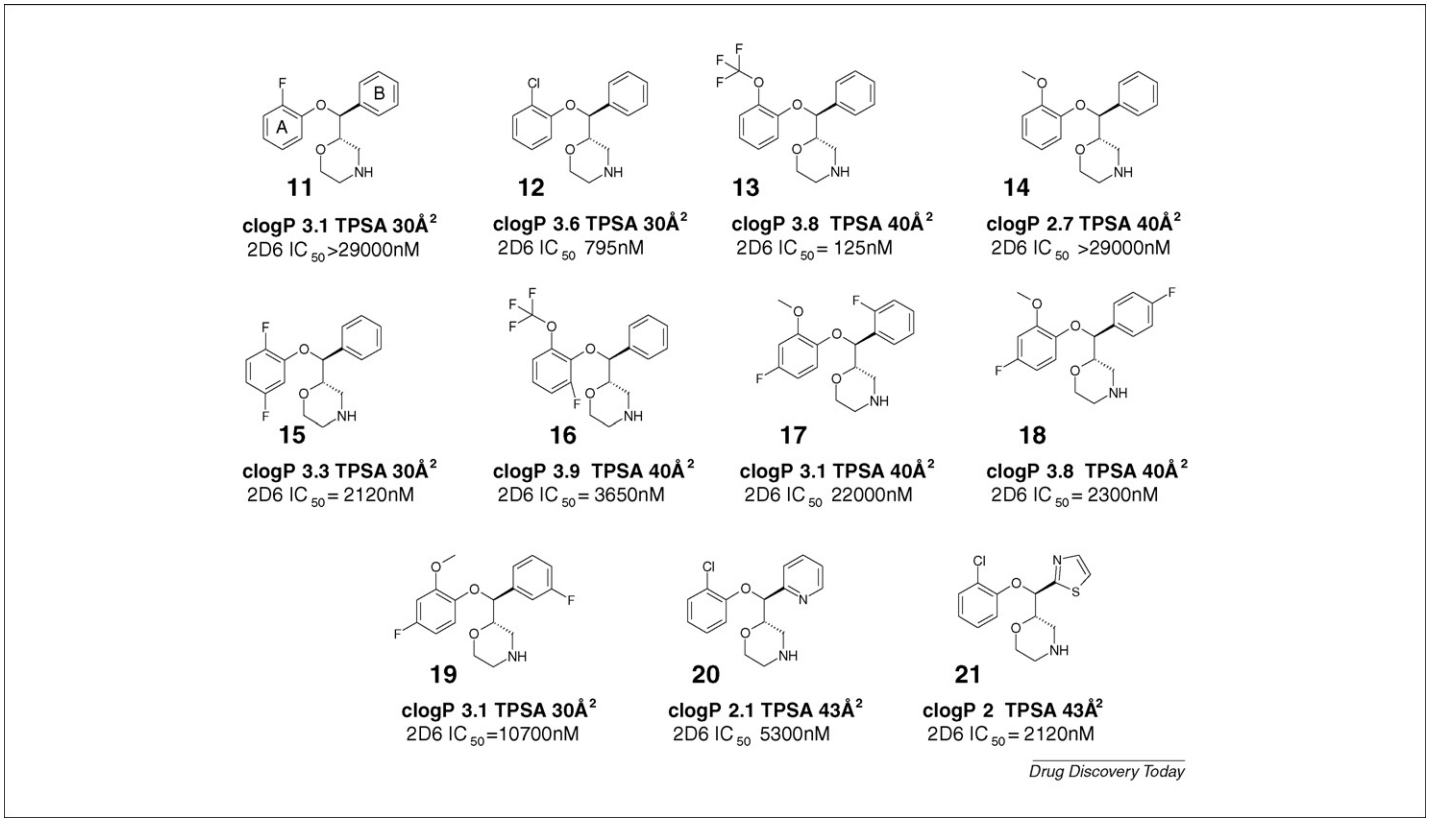

FIGURE 4

Non-heme binder SAR.

it is not always successful, as illustrated in Figure 5. Compound **22** was found to be mainly metabolized by CYP2D6 through oxidation of the benzylic ring, and via CYP3A4 through *N*-dealkylation. Blocking the CYP2D6 mediated pathway by replacing the 2,3-di-Me benzylic substituents with 2,3-di-Cl was successful leading to compound **23** for which *N*-dealkylation was identified to be the major route of metabolism. However, this metabolic pathway was also found to be mediated by CYP2D6 and not CYP3A4, which was contrary to the case for compound **22**. Blocking the *N*-dealkylation pathway by introduction of an amide group afforded compound **24** for which no metabolism was detected in *in vitro* microsomal preparations and as such quantitative assessment of CYP2D6 metabolism was not possible.

Researchers at Eli Lilly have also presented some interesting SAR whereby modulation of the pKa of an aryloxy phenylpropanamine by fluorination in the beta position resulted in a significant reduction in CYP2D6 metabolism. No structures have been published as yet [77].

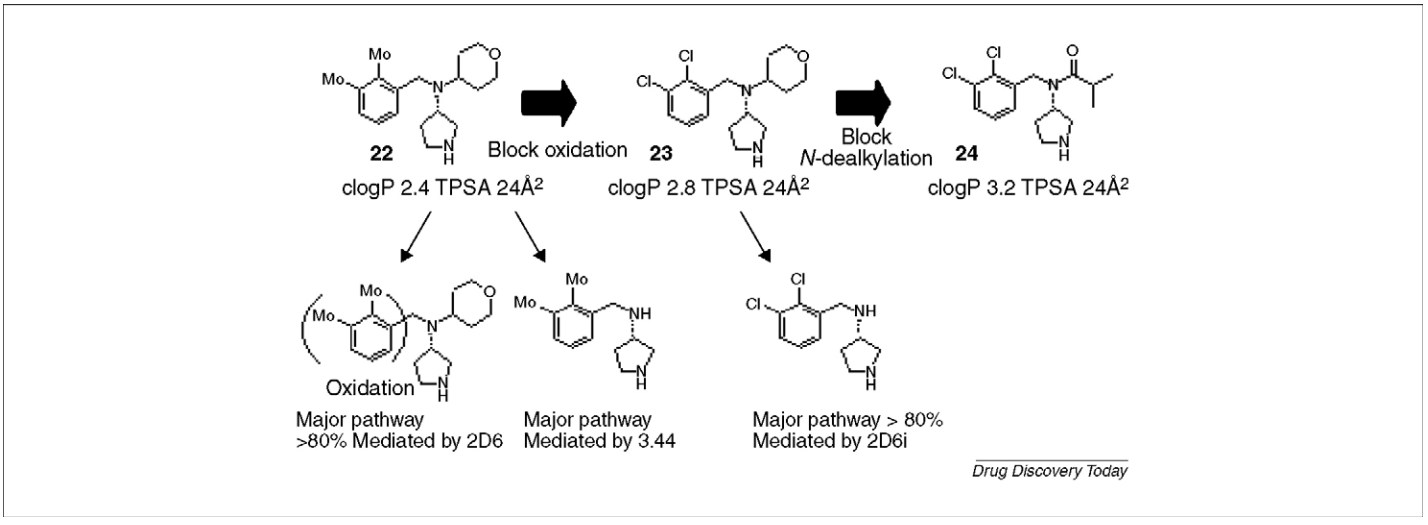

FIGURE 5

Metabolic pathway of compound **22** and **23** and strategy to design CYP2D6 metabolism out.

Summary

Owing to the polymorphic nature of CYP2D6, clinically significant issues can arise in CYP2D6 PM population when drugs rely on that enzyme either for clearance, or metabolism to an active metabolite. Available screening methods were discussed, to determine if the compound is likely to cause DDIs, or is likely to cause DDIs as a victim of inhibition of CYP2D6 by other compounds. Computational models have been described and examples of strategies to design out the CYP2D6 liabilities were given for both heme-binding and non-heme-binding compounds. The examples show that CYP2D6 interactions, metabolism or inhibition, can be overcome in drug discovery projects, although the strategies differ depending on the type of interactions the compounds make with the CYP2D6 enzyme.

Acknowledgements

The authors would like to David Gray for sharing the data generated in the morpholine series, James Mills for generating the CYP2D6 data set used for our analysis, Lyn Jones, Duncan Miller, David Price, Kevin Beaumont, Lourdes Cucurull–Sanchez, Duncan Armour and David Walsh for interesting discussions.

References

1 Nelson, D.R. *et al.* (1993) The P450 superfamily: update on new sequences, gene mapping, accession numbers, early trivial names of enzymes, and nomenclature. *DNA Cell Biol.* 12, 1–51
2 Nelson, D.R. *et al.* (1996) P450 superfamily: update on new sequences, gene mapping, accession numbers and nomenclature. *Pharmacogenetics* 6, 1–42
3 Zhou, S-F. *et al.* (2009) Substrate specificity, inhibitors and regulation of human cytochrome P450 2D6 and implications in drug development. *Curr. Med. Chem.* 16, 2661–2805
4 Williams, J.A. *et al.* (2004) Drug–drug interactions for UDP–glucuronosyltransferase substrates: A pharmacokinetic explanation for typically observed low exposure (AUCi/AUC) ratios. *Drug Metab. Dispos.* 32, 1201–1208
5 Hiratsuka, M. and Mizugaki, M. (2001) Genetic polymorphisms in drug-metabolizing enzymes and drug targets. *Mol. Genet. Metabol.* 73, 298–305
6 Aklillu, E. *et al.* (1996) Frequent distribution of ultrarapid metabolizers of debrisoquine in an Ethiopian population carrying duplicated and multiduplicated functional CYP2D6 alleles. *J. Pharmacol. Exp. Ther.* 278, 441–446
7 Mclellan, R.A. *et al.* (1997) Frequent occurrence of CYP2D6 gene duplication in Saudi Arabians. *Pharmacogenetics* 7, 187–191
8 Daly, A.K. *et al.* (1996) Nomenclature for human *CYP2D6* alleles. *Pharmacogenetics* 6, 193–201
9 Halling, J. *et al.* (2008) Genetic predisposition to Parkinson's disease: CYP2D6 and HFE in the Faroe islands. *Pharmacogenetics Genomics* 18, 209–212
10 Rostami-Hodjegan, A. *et al.* (1998) Meta-analysis of studies of the CYP2D6 polymorphism in relation to lung cancer and Parkinson's disease. *Pharmacogenetics* 8, 227–238
11 Ingelman-Sundberg, M. (2004) Pharmacogenetics of cytochrome P450 and its applications in drug therapy: the past, present and future. *Trends Pharmacol. Sci.* 25, 193–200
12 Strobl, G.R. *et al.* (1993) Development of a pharmacophore for inhibition of human liver cytochrome P-450 2D6: molecular modelling and inhibition studies. *J. Med. Chem.* 36, 1136–1145
13 Koymans, L.M.H. *et al.* (1992) A predictive model for substrates of cytochrome P-450-debrisoquine (2D6). *Chem. Res. Toxicol.* 5, 211–219
14 de Groot, M.J. *et al.* (1997) A refined substrate model for human cytochrome P450 2D6. *Chem. Res. Toxicol.* 10, 41–48
15 de Groot, M.J. *et al.* (1999) Novel approach to predicting P450 mediated drug metabolism. The development of a combined protein and pharmacophore model for CYP2D6. *J. Med. Chem.* 42, 1515–1524
16 de Groot, M.J. *et al.* (1999) A novel approach to predicting P450 mediated drug metabolism. CYP2D6 catalyzed *N*-dealkylation reactions and qualitative metabolite predictions using a combined protein and pharmacophore model for CYP2D6. *J. Med. Chem.* 42, 4062–4070
17 Samer, C.F. (2004) Cytochrome P450 2D6 genetic polymorphism: the rapid, the untrarapid, the intermediate and the slow. *Med. Hyg.* 62, 697–703
18 Ingelman-Sunberg, M. (2005) Genetic polymorphisms of cytochrome P450 2D6 (CYP2D6): clinical consequences, evolutionary aspects and functional diversity. *Pharmacogenetics J.* 6–13
19 Wijnen, P.A. *et al.* (2007) The Prevalence and clinical relevance of cytochrome P450 polymorphisms. *Aliment. Pharmacol. Ther.* 26, 211–219
20 Mulder, A.B. *et al.* (2001) Association of polymorphism in the cytochrome CYP2D6 and the efficacy and tolerability of simvastatin. *Clin. Pharm. Ther.* 70, 546–551
21 Kirchheiner, J. *et al.* (2004) Pharmacogenetics of antidepressants and antipsychotics: the contribution of allelic variations to the phenotype of drug response. *Mol. Psychiatry* 9, 442–473
22 Chou, W.H. *et al.* (2002) Extension of a pilot study: impact from the cytochrome P450 2D6 polymorphism on outcome and costs associated with severe mental illness. *Clin. Pharmacokinet.* 12, 453–470
23 Bijl, M.J. *et al.* (2009) Genetic variation in the CYP2D6 gene is associated with a lower heart rate and blood pressure in β-blocker users. *Clin. Pharm. Ther.* 85, 45–50
24 Beverage, J.N. *et al.* (2007) CYP2D6 polymorphisms and the impact on tamoxifen therapy. *J. Pharm. Sci.* 96, 2224–2231
25 McGinnity, D.F. *et al.* (2008) Integrated *in vitro* analysis for the *in vivo* prediction of cytochrome P450-mediated drug–drug interactions. *Drug Metab. Dispos.* 36, 1126–1134
26 Reese, M.J. *et al.* (2008) An *in vitro* mechanistic study to elucidate the desipramine/bupropion clinical drug–drug interaction. *Drug Metab. Dispos.* 36, 1198–1201
27 Rowland, M. and Matin, S.B. (1973) Kinetics of drug–drug interactions. *J. Pharmacokinetics Biopharm.* 1, 553–567
28 Kanamitsu, S. *et al.* (2000) Quantitative prediction of *in vivo* drug–drug interactions from *in vitro* data based on physiological pharmacokinetics: use of maximum unbound concentration of inhibitor at the inlet to the liver. *Pharm. Res.* 17, 336–343
29 Obach, R.S. *et al.* (2006) The utility of *in vitro* cytochrome P450 inhibition data in the prediction of drug–drug interactions. *J. Pharmacol. Exp. Ther.* 316, 336–348
30 Wrighton, S.A. *et al.* (2000) The human CYP3A subfamily: practical considerations. *Drug Metab. Rev.* 32, 339–361
31 Obach, R.S. *et al.* (2005) *In vitro* cytochrome P450 inhibition data and the prediction of drug–drug interactions: qualitative relationships, quantitative predictions, and the rank-order approach. *Clin. Pharmacol. Ther.* 78, 582–592
32 Jenkins, K.M. *et al.* (2004) Automated high throughput ADME assays for metabolic stability and cytochrome P450 inhibition profiling of combinatorial libraries. *J. Pharm. Biomed. Anal.* 34, 989–1004
33 Gao, F. *et al.* (2002) Optimizing higher throughput methods to assess drug–drug interactions for CYP1A2, CYP2C9, CYP2C19, CYP2D6, rCYP2D6, and CYP3A4 *in vitro* using a single point IC(50). *J. Biomol. Screen.* 7, 373–382
34 Moody, G.C. *et al.* (1999) Fully automated analysis of activities catalysed by the major human liver cytochrome P450 (CYP) enzymes: assessment of human CYP inhibition potential. *Xenobiotica* 29, 53–75
35 Weaver, R. *et al.* (2003) Cytochrome P450 inhibition using recombinant proteins and mass spectrometry/multiple reaction monitoring technology in a cassette incubation. *Drug Metab. Dispos.* 31, 955–966
36 Zientek, M. *et al.* (2008) Development of an *in vitro* drug–drug interaction assay to simultaneously monitor five cytochrome P450 isoforms and performance assessment using drug library compounds. *J. Pharmacol. Toxicol. Meth.* 58, 206–214
37 Cohen, L.H. *et al.* (2003) *In vitro* drug interactions of cytochrome p450: an evaluation of fluorogenic to conventional substrates. *Drug Metab. Dispos.* 31, 1005–1015
38 Williams, J.A. *et al.* (2003) Reaction phenotyping in drug discovery: moving forward with confidence? *Curr. Drug Metab.* 4, 527–534
39 Dickins, M. *et al.* (2007) Modelling and simulation of pharmacokinetic aspects of cytochrome p450-based metabolic drug–drug interactions. In *Comprehensive Medicinal Chemistry II*, (Vol. 5) (Taylor, J.B. and Triggle, D.J., eds) pp. 827–846, Elsevier Ltd.
40 Crespi, C.L. (1995) Xenobiotic-metabolizing human cells as tools for pharmacological and toxicological research. In *Advances in Drug Research* (Meyer, U.A. and Testa, B., eds), pp. 179–235, Academic Press
41 Proctor, N.J. *et al.* (2004) Predicting drug clearance from recombinantly expressed CYPs: intersystem extrapolation factors. *Xenobiotica* 34, 151–178

42 Rostami-Hodjegan, A. and Tucker, G.T. (2007) Simulation and prediction of *in vivo* drug metabolism in human populations from *in vitro* data. *Nat. Rev. Drug Discov.* 6, 140–148

43 Dickinson, G.L. *et al.* (2007) Incorporating *in vitro* information on drug metabolism into clinical trial simulations to assess the effect of CYP2D6 polymorphism on pharmacokinetics and pharmacodynamics: dextromethorphan as a model application. *J. Clin. Pharmacol.* 47, 175–186

44 Williams, P.A. *et al.* (2000) Mammalian microsomal cytochrome P450 monooxygenase: structural adaptations for membrane binding and functional diversity. *Mol. Cell.* 5, 121–131

45 Koymans, L.M.H. *et al.* (1993) A preliminary 3D model for cytochrome P450 2D6 constructed by homology model building. *J. Comput. Aided Mol. Des.* 7, 281–289

46 de Groot, M.J. *et al.* (1996) A three-dimensional protein model for human cytochrome P450 2D6 based on the crystal structures of P450 101, P450 102 and P450 108. *Chem. Res. Toxicol.* 9, 1079–1091

47 Modi, S. *et al.* (1996) A model for human cytochrome P_{450} 2D6 based on homology modeling and NMR studies of substrate binding. *Biochemistry* 35, 4540–4550

48 Lewis, D.F.V. *et al.* (1997) Molecular modelling of cytochrome P4502D6 (CYP2D6) based on an alignment with CYP102: structural studies on specific CYP2D6 substrate metabolism. *Xenobiotica* 27, 319–340

49 Kirton, S.B. *et al.* (2002) Impact of incorporating the CYP2C5 crystal structure into comparative models of cytochrome P450 2D6. *Proteins Struct. Funct. Genet.* 49, 216–231

50 Venhorst, J. *et al.* (2003) Homology modeling of rat and human cytochrome P450 2D (CYP2D) isoforms and computational rationalization of experimental ligand-binding specificities. *J. Med. Chem.* 46, 74–86

51 Rowland, P. *et al.* (2006) Crystal structure of human cytochrome P450 2D6. *J. Biol. Chem.* 281, 7614–7622

52 Strobl, G. (1991) Entwicklung von strukturmodellen für substrate und inhibitoren von cytochrom P-450IID1 mit hilfe von molecular modeling und in-vitro-hemmungsmessungen. *GSF Forschungszentrum für Umwelt und Gesundheit GmbH.*

53 Strobl, G. and Wolff, T. (1992) Structural models for inhibitors and substrates of cytochrome P-450IID6 based on molecular modeling analysis. In *Cytochrome P450 biochemistry and biophysics* (Archakov, A.I. and Bachmanova, G.I., eds), pp. 736–738, INCO—TNC Joint Stock Company

54 Manuscript in preparation

55 Wolff, T. *et al.* (1985) Substrate specificity of human liver cytochrome P-450 debrisoquine hydroxylase probed using immunochemical inhibition and chemical modeling. *Cancer Res.* 45, 2116–2122

56 Meyer, U.A. *et al.* (1986) The molecular mechanism of two common polymorphisms of drug oxidation. Evidence for functional changes in cytochrome P-450 isozymes catalysing bufuralol and mephenytoin oxidation. *Xenobiotica* 16, 449–464

57 Islam, S.A. *et al.* (1991) A three-dimensional molecular template for substrates of human cytochrome P450 involved in debrisoquine 4-hydroxylation. *Carcinogenesis* 12, 2211–2219

58 de Groot, M.J. *et al.* (1995) Computer prediction and experimental validation of cytochrome P450-2D6 dependent oxidation of GBR 12909 (1-[2-[bis(4-fluorophenyl)methoxy]ethyl]-4-(3-phenylpropyl)piperazine). *Drug Metab. Dispos.* 23, 667–669

59 de Groot, M.J. *et al.* (1997) Extension of a predictive substrate model for human cytochrome P4502D6. *Xenobiotica* 27, 357–368

60 Snyder, R. *et al.* (2002) Three-dimensional quantitative structure activity relationship for Cyp2d6 substrates. *Quant. Struct. Act. Relat.* 21, 357–368

61 Ekins, S. *et al.* (1999) Three and four dimensional-quantitative structure activity relationship (3D/4D-QSAR) analyses of CYP2D6 inhibitors. *Pharmacogenetics* 9, 477–489

62 Ekins, S. and Wrighton, S.A. (2001) Application of *in silico* approaches to predicting drug–drug interactions. *J. Pharmacol. Toxicol. Methods* 45, 65–69

63 Ekins, S. *et al.* (2003) Generation and validationof rapid computational filters for CYP2D6 and CYP3A4. *Drug. Metab. Dispos.* 31, 1077–1080

64 Balakin, K.V. *et al.* (2004) Quantitative structure-metabolism relationship modeling of metabolic *N*-dealkylation reaction rates. *Drug Metab. Dispos.* 32, 1111–1120

65 Burton, J. *et al.* (2006) Recursive partitioning for the prediction of cytochromes P450 2D6 and 1A2 inhibition: importance of the quality of the dataset. *J. Med. Chem.* 49, 6231–6240

66 Gleeson, M.P. *et al.* (2007) Generation of *in silico* cytochrome P450 1A2, 2C9, 2C19, 2D6, and 3A4 inhibition QSAR models. *J. Comput. Aided Mol. Des.* 21, 559–573

67 Jensen, B.F. *et al.* (2007) *In silico* prediction of cytochrome P450 2D6 and 3A4 inhibition using Gaussian kernel weighted k-nearest neighbor and extended connectivity fingerprints, including structural fragment analysis of inhibitors versus noninhibitors. *J. Med. Chem.* 50, 501–511

68 Sciabola, S. *et al.* (2007) Pharmacophoric fingerprint method (TOPP) for 3D-QSAR modeling: application to CYP2D6 metabolic stability. *J. Chem. Inf. Model.* 47, 76–84

69 Appiah-Opong, R. *et al.* (2008) Structure-activity relationships for the inhibition of recombinant human cytochromes P450 by curcumin analogues. *Eur. J. Med. Chem.* 43, 1621–1631

70 Roy, P.P. and Roy, K. (2009) QSAR studies of CYP2D6 inhibitor aryloxypropanolamines using 2D and 3D descriptors. *Chem. Biol. Drug. Des.* 73, 442–455

71 Kemp, C.A. *et al.* (2004) Validation of model of cytochrome P450 2D6: an *in silico* tool for predicting metabolism and inhibition. *J. Med. Chem.* 47, 5340–5346

72 Keizers, P.H. *et al.* (2005) Metabolic regio- and stereoselectivity of cytochrome P450 2D6 towards 3,4-methylenedioxy-*N*-alkylamphetamines: *in silico* predictions and experimental validation. *J. Med. Chem.* 48, 6117–6127

73 Vaz, R.J. *et al.* (2005) A 3D-QSAR model for CYP2D6 inhibition in the aryloxypropanolamine series. *Bioorg. Med. Chem. Lett.* 15, 3815–3820

74 Gleeson, M.P. (2008) Generation of a set of simple, interpretable ADMET rules of thumb. *J. Med. Chem.* 51, 817–834

75 McMasters, D.R. *et al.* (2007) Inhibition of recombinant cytochrome P450 isoforms 2D6 and 2C9 by diverse drug-like molecules. *J. Med. Chem.* 50, 3205–3213

76 Wakenhut, F. *et al.* (2008) *N*-Benzyl-*N*-(pyrrolidin-3-yl)carboxamides as a new class of selective dual serotonin/noradrenaline reuptake inhibitors. *Bioorg. Med. Chem. Lett.* 18, 4308–4311

77 Boulet, S.L. *et al.* (2004) Effect of hydroxylation and fluorination of aryloxy phenylpropanamine serotonin and norepinephrine reuptake inhibitors on CYP450 2D6 dependant metabolism. *228th ACS National Meeting*, ACS